

# Electromigration issues in lead-free solder joints

Chih Chen · S. W. Liang

Published online: 8 September 2006  
© Springer Science+Business Media, LLC 2006

**Abstract** As the microelectronic industry advances to Pb-free solders due to environmental concerns, electromigration (EM) has become a critical issue for fine-pitch packaging as the diameter of the solder bump continues decreasing and the current that each bump carries keeps rising owing to higher performance requirement of electronic devices. As stated in 2003 International Technology Roadmap for Semiconductors (ITRS), the EM is expected to be the limiting factor for high-density packages. This paper reviews general background of EM, current understanding of EM in solder joints, and technical hurdles to be addressed as well as possible solutions. It is found that the EM lifetimes of Pb-free solder bumps are between the high-Pb and the eutectic composition under the same testing condition. However, our simulation results show that the electrical and thermal characteristics remain essentially almost the same during accelerated EM tests when the Pb-containing solders are replaced by Pb-free solders, suggesting that the melting points of the solders are likely the dominant factor in determining EM lifetimes. The EM behavior in Pb-free solder is a complicated phenomenon as multiple driving forces coexist in the joints and each joint contains more than four elements with distinct susceptibility to each driving force. Therefore, atomic transport due to electrical and thermal driving forces during EM is also investigated. In addition, several approaches are presented to reduce undesirable current crowding and Joule heating effects to improve EM resistance.

## 1 Overview of the background

Electromigration (EM) has been the most persistent reliability issue in interconnects of microelectronic devices [1]. It is the mass transport of atom driven by combined forces of electric field and charge carriers. As illustrated in Fig. 1, the drifting electrons collide with atoms causing one of the atoms to exchange position with neighboring vacancy during current stressing. The necessary current density to initiate the movement of atom is defined as the threshold current density. Due to the relentless drive for miniaturization of portable devices, the interconnects for those devices are scaling down successively, whereas the required performance continues increasing. As a result, the current density in the interconnect rises continuously with each generation, making the EM a critical reliability issue ever. After stressing for extended time, atoms in interconnects accumulate on the anode end and voids appear on the cathode side, resulting in open failure eventually. In general, the average drift velocity of atom due to EM is given by Huntigton and Grone [2]:

$$v = \frac{J}{C} = BeZ^* \rho j = \left( \frac{D_0}{kT} \right) eZ^* \rho j \exp\left( \frac{-E_a}{kT} \right) \quad (1)$$

where  $J$  is the atom flux,  $C$  is the density of metal ions,  $B$  is the mobility,  $k$  is the Boltzmann's constant,  $T$  is the absolute temperature,  $eZ^*$  is the effective charge of the ions,  $\rho$  is the metal resistivity,  $j$  is the electrical current density,  $E_a$  is the activation energy of diffusion, and  $D_0$  is the prefactor of diffusion constant.

Recently, with stringent environmental regulation, lead-free solders have been adopted to replace

C. Chen (✉) · S. W. Liang  
Department of Material Science & Engineering, National  
Chiao Tung University, Hsin-chu 30050, Taiwan, ROC  
e-mail: chih@faculty.nctu.edu.tw

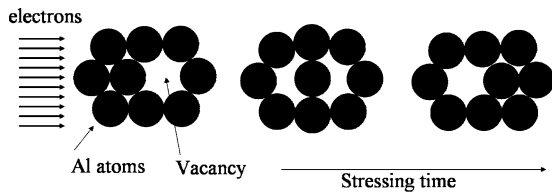


**Fig. 1** Schematic diagram showing the diffusion process due to wind force of electrons during EM test. The current density should be high enough to trigger the diffusion process

Pb-containing ones in microelectronics industry. Concurrently, the flip-chip solder joint has assumed the leadership role for high-density packaging in the microelectronic industry as thousands of solder bumps are fabricated into one single chip. To meet higher demand for device performance, the input/output numbers is expected to increase while the dimension of each individual joint is shrunk accordingly. To date, each bump measures at 100  $\mu\text{m}$  or less in diameter. The design rule of packaging dictates that each bump is likely to carry current of 0.2–0.4 A [1], which amounts to current density in the range of  $2 \times 10^3 \text{ A/cm}^2$  to  $1 \times 10^4 \text{ A/cm}^2$ . During device operation, these solder joints frequently reach a temperature as high as 100°C, approximately 77% of the absolute melting temperatures of most Pb-free solder candidate materials including eutectic SnAgCu and SnAg. Understandably, with such high current densities and operation temperatures, facile diffusion of atoms in the lattice is foreseeable. This renders EM a daunting reliability issue for Pb-free implementation [3].

## 2 Current status

Previous studies on EM of flip chip solder bumps focused mainly on eutectic SnPb solders. In 1998, Brandenburg et al. first reported the failure of eutectic SnPb solder joints under current stressing of 0.625 A at 150°C for 600 h [4]. Tu et al. performed systematic studies and provided insightful reasoning on the EM in Pb-containing solder. They identified that the Sn atoms are the principal diffusion entities at room temperature, whereas Pb atoms dominate at 150°C [5, 6]. In addition, they discovered that the effect for current crowding is more pronounced in the flip-chip solder joints for its unique line-to-bump structure [7]. They performed two-dimensional simulation and the results showed that the local current density at the solder near the entrance of the Al trace was at least 10 times greater than the average value, a number obtained by assuming uniform current spreading in the passivation opening or under-bump-metallization (UBM) opening.

This finding is significant in pinpointing possible location for failure event in EM. Figure 2(a) depicts a three-dimensional (3D) schematic for a solder joint with line-to-bump structure consisting Al trace of 34  $\mu\text{m}$  in width and 1.5  $\mu\text{m}$  in thickness, solder bump with a UBM opening of 120  $\mu\text{m}$  in diameter, as well as Cu line with 80  $\mu\text{m}$  in width and 25  $\mu\text{m}$  in thickness on the substrate side. In this design the cross-section of the Al trace is about 220 times smaller than that of the UBM opening. When the joint was subjected to a current of 0.567 A, the current density in the Al trace reached  $1.1 \times 10^6 \text{ A/cm}^2$ , whereas the average current density in the UBM opening was only  $5.0 \times 10^3 \text{ A/cm}^2$ . However, our 3D simulation showed that in thin film UBM configuration, close proximity to the entrance of the Al trace the local current density of the solder could achieve  $1.24 \times 10^5 \text{ A/cm}^2$  [8], a value that is 24.8 times greater than the average  $5.0 \times 10^3 \text{ A/cm}^2$  one would expect. Among the possible materials used in the joint, solder is considered to exhibit the lowest resistance to EM [1]. Reasonably, we can conclude that solder in this specific location experiences larger electron wind force at a relatively high temperature to its

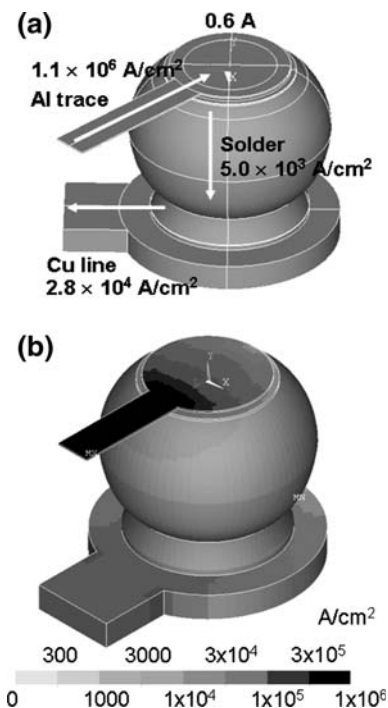
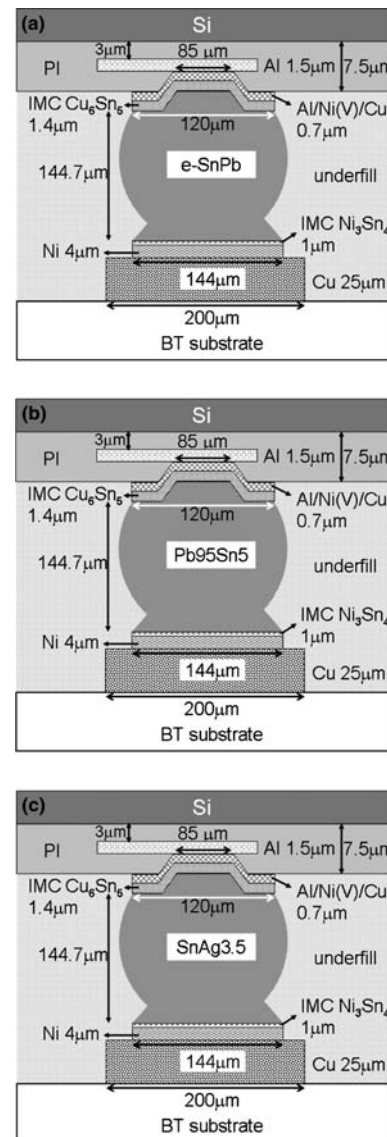


**Fig. 2** (a) The 3D schematic for a solder joint with the line-to-bump structure with a 34- $\mu\text{m}$  wide and 1.5- $\mu\text{m}$  thick Al trace. When the joint was applied by 0.567 A, the average current densities in the Al trace, solder bump, and Cu line are shown in the figure. (b) Tilt-view showing the 3D current density distribution in the solder joint when it is powered by 0.57 A. Current crowding occurred very seriously in the junction of the Al trace and the solder bump

melting point. Therefore, flux divergence of mass transport occurs substantially resulting in the formation of catastrophic voids which are directly responsible for interconnect failure.

Besides the current crowding effect, Joule heating also plays a crucial role in the failure mechanism. Recently, findings indicate that a hot-spot exists near the entrance point of the Al trace due to localized Joule heating effect [9]. The resultant temperature difference between the hot-spot and the average temperature in solder can reach 9.4°C under 0.8 A of current flow as shown in Fig. 2(a). In 2003, Ye et al. reported the observation of voids on the chip/anode side [10], and they attributed the void development to thermomigration (TM) as thermal gradient of 1500°C/cm across the solder bump was established during accelerated EM tests. Similarly, Huang et al. found that Sn atom migrates towards the hot side but Pb atom migrates to the cold end [11]. The occurrence of TM during EM complicates the reliability issue. On the other hand, the EM for compositions of the high-Pb and eutectic SnPb solder joints with 5- $\mu\text{m}$  Cu UBM were studied and concluded that the dissolution of the Cu UBM at the current crowding region was primarily responsible for the failure of the joints [12, 13]. The dissolution rate at the current crowding region was accelerated because of higher wind force in combination with elevated temperature for facile diffusion.

Unfortunately, the mean-time-to-failure (MTTF) for Pb-free SnAgCu and SnAg solders joints are shorter than that of the high-Pb solders under the same stressing conditions. Since high-Pb solders are currently adopted for high-density packages, such as microprocessors, EM would be a critical issue for Pb-free implementation. In 2004, Wu et al. demonstrated that the MTTF of SnAg4.0Cu0.5 solder is about five times longer than that of the eutectic SnPb solder, yet is somewhat shorter than that of the high-Pb solder [14]. Gee et al. and Choi et al. also reported that the MTTF of eutectic SnAgCu solder joints was better than that of eutectic SnPb solder joints with the same UBM under the same stressing conditions [15, 16]. To elucidate how the current density and temperature distribute during current stressing, 3D electrothermal-coupled modeling was performed on the solder joints with identical configuration but with different solders materials. They include eutectic SnPb, high-Pb SnPb95 and eutectic SnAg. Figure 3(a)–(c) shows the cross-sectional schematics for these three models. The passivation opening was 85  $\mu\text{m}$  in diameter and the UBM opening was 120  $\mu\text{m}$  in diameter. The dimensions of the Al trace and the Cu line were consistent with those in Fig. 2. Relevant materials characteristics of materi-

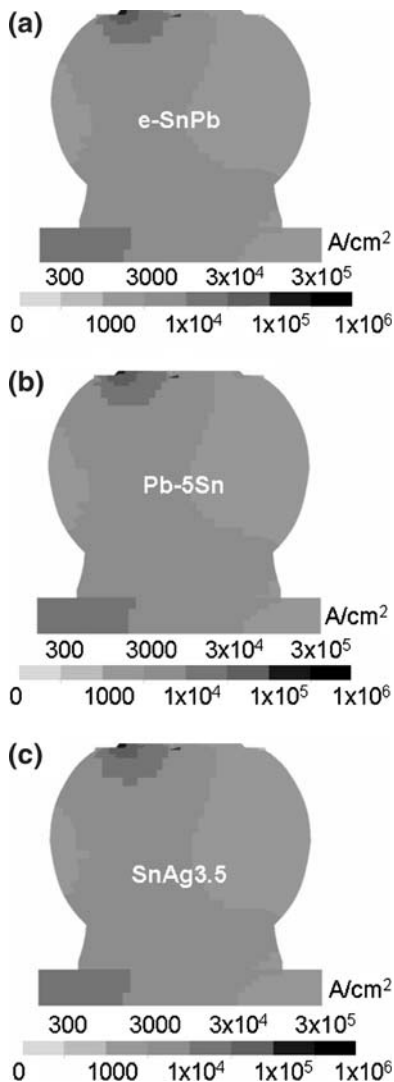


**Fig. 3** The cross-sectional schematic showing the three constructed models for electrical–thermal coupled simulation: (a) Eutectic SnPb solder joint; (b) high-Pb solder joint; (c) Eutectic SnAg solder joints. All the features remain are identical except the solder materials

als used in this simulation are provided in Table 1. The dimension of the Si chip was 7.0 mm  $\times$  4.8 mm with thickness of 290  $\mu\text{m}$ . The dimension of the bismaleimide triazine (BT) substrate was 5.4 mm in width, 9.0 mm in length, and 480  $\mu\text{m}$  in thickness. The bottom of the BT substrate was maintained at 70°C and the convection coefficient was set at 10 W/m<sup>2</sup>°C in a 25°C ambient temperature. Constant current of 0.6 A was applied through the Cu lines on the BT substrate [9]. Among these three solders, the Pb-free SnAg possesses the lowest electrical resistivity and thermal conductivity of 12.3  $\mu\Omega\text{ cm}$  and 33 W/m K respectively. Figure 4(a)–(c) displays the current density

**Table 1** The materials properties used in this paper

Materials	Thermal conductivity (W/m K)	Resistivity (mΩ cm)	Temperature coefficient of resistivity (K <sup>-1</sup> )
Al	238	2.7	$4.2 \times 10^{-3}$
Al/Ni(V)Cu	166.6	29.54	$5.6 \times 10^{-3}$
Cu6Sn5	34.1	17.5	$4.5 \times 10^{-3}$
Pb-5Sn	63	19	$4.2 \times 10^{-3}$
e-SnPb	50	14.6	$4.4 \times 10^{-3}$
SnAg3.5	33	12.3	$4.6 \times 10^{-3}$
Ni3Sn4	19.6	28.5	$5.5 \times 10^{-3}$
Ni	76	6.8	$6.8 \times 10^{-3}$
Cu	403	1.7	$4.3 \times 10^{-3}$
Si	147	–	–
BT	0.7	–	–
Underfill	0.55	–	–
PI	0.34	–	–

**Fig. 4** The simulation results showing the current density distribution under 0.6 A in: (a) Eutectic SnPb solder bump; (b) high-Pb solder bump; (c) Eutectic SnAg solder bump

distribution in the solder joints under the stress current of 0.6 A. The distribution profiles remain essentially the same. The maximum current density were  $1.03 \times 10^5$  A/cm<sup>2</sup>,  $9.42 \times 10^4$  A/cm<sup>2</sup>,  $1.11 \times 10^5$  A/cm<sup>2</sup> for the eutectic SnPb, high-Pb, and the eutectic SnAg solders, respectively. The Pb-free solder exhibits the highest current crowding effect because of its lowest electrical resistivity. Figure 5(a)–(c) illustrates the temperature distribution in the solder bumps. The solders near the entrance point of the Al trace all show higher temperature than the rest of the solder. Figure 6(a)–(c) shows the cross-sectional views for the temperature distribution. The results indicate the existence of hot-spots in these solder bumps. The hot-spot temperature was 100.0°C, 103.6°C, and 105.4°C, respectively, whereas the average temperature was 95.9°C, 99.2°C, and 98.9°C for the eutectic SnPb, high-Pb, and the eutectic SnAg solder. The Pb-free solder experienced the highest Joule heating effect, which may be due to limited intrinsic capability for heat dissipation and highest current crowding effect. Since the majority of heat source was Al trace [17], lower resistivity of the Pb-free solders did not necessarily render a smaller Joule heating effect. The simulation results are summarized in Table 2.

So far, our data demonstrate that the current crowding and Joule heating effects in Pb-free SnAg solder bump are marginally worse than those in eutectic SnPb solder bump, as shown in Figs. 4 and 5. Nevertheless, the Pb-free solder exhibits far better EM resistance than that of the eutectic SnPb [18]. This surprising improvement may be attributed to the reduced diffusivity for Pb-free solder as its melting point is approximately 50°C higher than that of the eutectic SnPb solder. As a result, the rate of void formation is much lower than that in the eutectic solder. In addition, the highest MTTF for the high-Pb solder may be

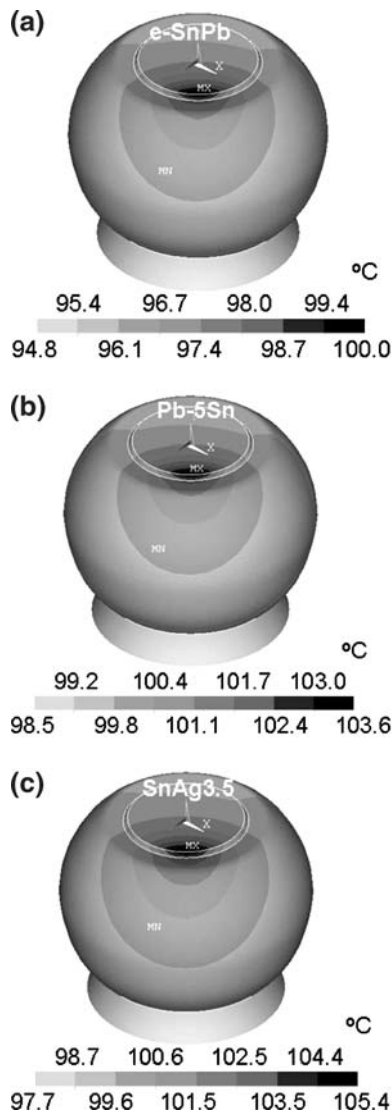


**Fig. 5** The simulation results showing the temperature distribution under 0.6 A in: (a) Eutectic SnPb solder bump; (b) high-Pb solder bump; (c) Eutectic SnAg solder bump. A hot-spot exists near the entrance point of the Al trace

mainly due to its higher liquidus temperature of about 320°C. For example, at stressing temperature of 150°C, it is 93%, 86%, and 71% of the melting points for the eutectic SnPb, eutectic SnAg, and high-Pb solders, respectively. Typically, at melting point metal atoms exhibit a diffusivity of  $10^5$  cm<sup>2</sup>/s to  $10^7$  cm<sup>2</sup>/s in nature. Therefore, it is prudent to assume that the diffusivity of the Pb-free solder would fall somewhere in between these two Pb-containing solders. This is in accordance to the findings that the EM resistance of Pb-free solder is higher than that of the eutectic SnPb solder, but lower than that of the high-Pb solder.

Likewise, interfacial metallurgical reaction becomes crucial in Pb-free solder joints during current stressing,

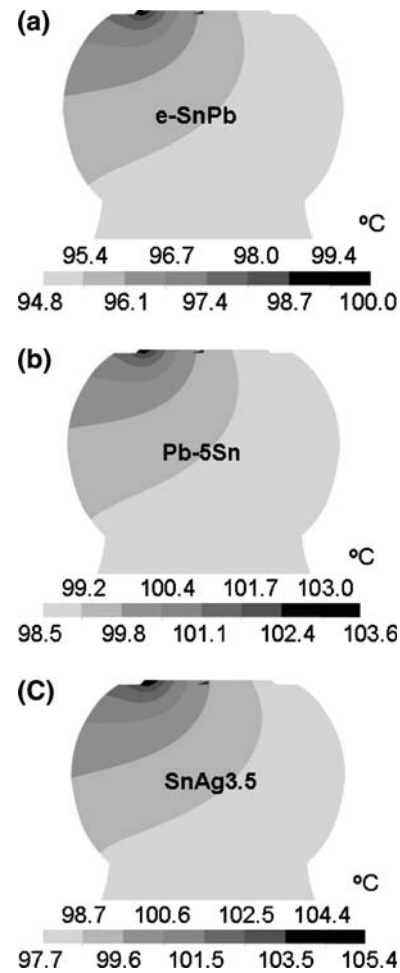


**Fig. 6** The cross-sectional view of the results in Fig. 5. (a) Eutectic SnPb solder bump; (b) high-Pb solder bump; (c) Eutectic SnAg solder bump under 0.6 A. The solder on the Si side is hotter than that on the substrate side. Thermal gradient was built across the solder bump

especially at critical stressing conditions when the solder and the UBM undergo a solid state aging process during EM. It is reported that the Cu–Sn IMC may grow over 13 μm for Pb-free SnAg solder after aging at 170°C for 1500 h [19]. Electron wind force is likely to enhance the dissolution of the UBM materials on the cathode end, and the erosion of the latter may lead to the failure of the solder joints [12, 13]. Thus, the interfacial reaction appears to be the critical factor for the EM of Pb-free solders. Due to the spalling issue for thin-film UBM in Pb-containing and Pb-free solders [3, 20], thick-film Cu or Ni UBM has been adopted for the Pb-free solder joints. This not only solves the spalling problem, but also prolongs the EM lifetime. This point will be discussed later.

The interfacial reactions are accelerated by the stressing current during EM. Chen et al. first investigated the effect of electrical current on interfacial

**Table 2** The simulation results on maximum current density, hot-spot and average temperatures, and thermal gradient for the high-Pb, eutectic SnPb, and SnAg solders

	Maximum current density (A/cm <sup>2</sup> )	Hot-spot (°C)	Average temperature (°C)	Thermal gradient (°C/cm)
Pb95Sn5	$9.42 \times 10^4$	103.6	99.2	246.9
e-SnPb	$1.03 \times 10^5$	100	95.5	259.2
SnAg3.5	$1.11 \times 10^5$	105.4	98.9	398.7

reactions in solder systems in 1998 [21], and they found that the flow of electrons may enhance or inhibit the growth of the intermetallic compound. For SnPb solder joints, the Pb atoms are the dominant diffusing species when the joints are stressed above 100°C. Figure 7 depicts the schematic for two bumps with opposite current directions. Hence, the Pb atoms move to the chip/anode and substrate/anode sides during current stressing. This phase segregation may enhance the dissolution of the UBM in the chip/cathode end because excess Sn atoms accumulate there. Yet, it prevents the UBM on the chip/anode side from reacting with the solder as the Pb atoms are unlikely to form IMC with Cu or Ni UBM. For Pb-free solders, the interfacial reaction on the chip/anode side becomes noticeable. Extensive IMC formation on the chip/anode during stringent stressing conditions for SnAg solder joints has been reported in literature [22, 23]. Nickel atoms on the substrate/cathode migrated to the chip/anode side and subsequently formed IMC there, a potential failure site. At a reduced stressing current and temperature, the joints failed at chip/cathode side. Unfortunately, the failure modes for thick-film Cu (over 10 μm) or Ni UBM are not yet clear.

Under the electrical (EM) and thermal (TM) driving forces, the diffusion of atoms in the solder joint are rather complicated. Figure 8(a) illustrates the direction of the movement of the atoms under these two driving forces during an accelerated EM test. The simulation assumes a Pb-containing solder in combination with Cu and Ni serving as the UBM material in the chip side and metallization material in the substrate side. In

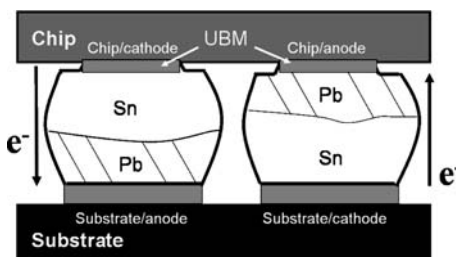


**Fig. 7** Schematic drawing showing the polarity effect of during EM testing at temperature higher than 100°C. Lead atoms accumulated on the chip/anode and substrate/anode ends

addition, electrons drift upwards in Bump 1, whereas they move downwards in Bump 2. Bump 3 acts as a control sample without passage of current but it undergoes the same thermal history as Bump 1 and 2. During EM testing, the Si die is the hot end due to the excessive Joule heating in the Al trace. For Pb-containing solder bumps, open failure occurs in the chip/cathode of Bump 2 since flux divergence takes place to greater degree at this end. As shown in the Fig. 8(a), due to the apparent current crowding effect in the chip side [8], Sn, Pb, and Cu atoms will migrate away from the chip/cathode end. Furthermore, the built-in thermal gradient also drives the Pb atoms to the substrate side [11]. On the other hand, only an opposite flux of Sn due the thermomigration flows to the chip/cathode end [11]. At testing temperatures above 100°C, Pb atoms are the predominant diffusion species. Thus, both EM and TM forces remove atoms from the chip end to the substrate side in this bump with the net result of void formation in the chip/cathode end. Also, the Pb segregation in the substrate/anode side is quite noticeable after current stressing for extended time [24].

For Bump 1 with upward electron flow, SnPb solder will migrate to the chip/anode side. However, the force

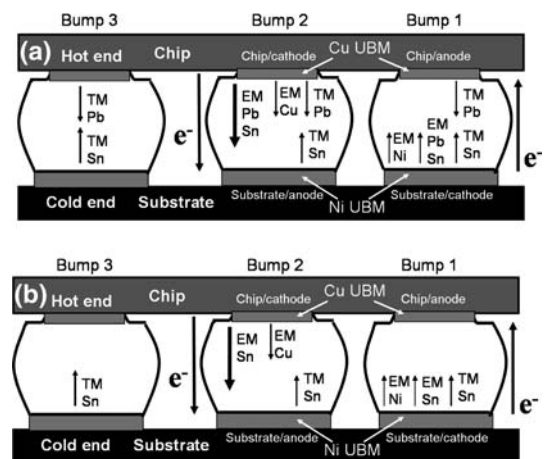


**Fig. 8** Diffusion of atoms in solder bumps due to EM and TM forces for: (a) Pb-containing solder bumps; (b) Pb-free solder bumps

is negligible compared with that in Bump 2, since there is almost no current crowding effect in the substrate side due to the large cross-section of the Cu line in the substrate [8]. In addition, Ni atoms in the substrate side will migrate toward chip/anode side due to the EM force [22, 23], and Sn atoms will also diffuse to the chip/anode side under TM force. In contrast, the Pb atoms will move to the substrate/cathode end due to TM force. Thus, the EM and TM forces counteract each other at higher stressing temperatures when the Pb atoms are the dominant diffusion species. Huang *et al.* shown that a thermal gradient of 1000°C/cm would provide comparable magnitude of driving force to that of EM force, triggering notable thermomigration in the solder bump [11].

For Bump 3 without passage of any current, the built-in thermal gradient may be close to those in Bump 1 and Bump 2 if the Bump 3 is close to them. Because the heat conduction of Si is appreciable, the Bump 3 may experience similar amount of Joule heating as Bump 1 and 2 do [25]. Hence, the temperature of the solder near the Si die is expected to be higher than that in the substrate side, causing a thermal gradient across the solder joint even without current passage. In addition, since EM force is absent in Bump 3 because there was no current passing through, it offers a great opportunity to decouple the atom migration due to the EM and the TM forces [11]. As depicted in Fig. 8(a), the built-in thermal gradient drives the Pb atoms near the chip side to the substrate side, whereas it triggers the Sn atoms in the substrate side moving to the chip side. The migration of atoms in this bump is mainly attributed to the TM force. It is noteworthy that the current should be sufficiently high to produce a steep thermal gradient across the solder joint. Applied current larger than 1 A was used in those studies that reported thermomigration so far [10, 11]. At lower stressing temperatures, Sn atoms are the predominant diffusion species. For Bump 1, both EM and TM forces propel the Sn atoms towards the chip/anode side. For Bump 2, EM failure may be inhibited to some extent since Sn fluxes due to the EM and TM force are in the favorable direction.

As for Pb-free solder bumps including eutectic SnAgCu and SnAg, Sn atoms are the leading diffusion species during EM. Therefore, the diffusion behaviors driven by EM and TM forces become relatively straightforward, as shown in Fig. 8(b). For Bump 1, both Sn and Ni atoms migrate to the chip/anode end due to EM force, and the TM force also promotes the Sn atoms to that end. As for Bump 2, The EM force drives the Sn and Cu down to substrate/anode end, whereas the TM force prods Sn atom in the opposite

direction. Therefore, the damage caused by EM damage may be limited if the thermal gradient is sufficiently large. In comparison, there is only one force acting on the Bump 3 because it had no electrical current pass through, and Sn atoms are driven toward the chip end. Nevertheless, experimental results are unavailable for thermomigration in Pb-free solders to date.

### 3 Problems that still need to be addressed and the suggestions for solving them

#### 3.1 Modification of MTTF equation

From engineering point of view, modification of MTTF equation for the use of flip-chip in solder joints is urgently needed. The equation of mean-time-to-failure (MTTF) for Al and Cu interconnects is typically expressed as below [26]:

$$\text{MTTF} = A \frac{1}{j^n} \exp\left(\frac{Q}{kT}\right) \quad (1)$$

where  $A$  is a constant,  $j$  is the average current density,  $n$  is a model parameter for current density,  $Q$  is the activation energy,  $k$  is the Boltzmann's constant, and  $T$  is the average bump temperature. As stated above, current crowding and Joule heating effect occurs substantially in flip-chip solder joints, and the failure is usually initiated at the current crowding region in solder, which happens to be the hot-spot. Voids start to form here, or the UBM dissolves quickly at the region. Therefore, the equation should be revised to include current crowding and Joule heating effects for consideration during accelerated EM tests. Tu *et al.* proposed that the term  $j^{-n}$  in the equation needs to be revised to  $(cj)^{-n}$  in order to capture the high current crowding effect in the solder joints [16]. Moreover, the temperature factor is later adapted to  $(T + \Delta T)$  to account for appreciable Joule heating effect during the accelerated EM test. Further effort is necessary to identify the precise current density term. Since the hot-spot is present, we suggest revising the temperature term to use the hot-spot temperature in predicting the MTTF of the solder joints. We believe that the Joule heating effect needs to be measured with greater accuracy. Otherwise, the MTTF would be underestimated.

#### 3.2 Relieving current crowding and Joule heating effects

Current crowding and Joule heating effects play vital role in the failure of flip-chip solder joints. Hence,

relieving of these undesirable influences is expected to improve the EM resistance significantly. As delineated by Black's equation, reducing the local current density by 50% may extend the MTTF by four times if we take  $c_j$  term to be the maximum current density and  $n$  to be equal to 2. In addition, the MTTF increases exponentially with decreasing bump/hot-spot temperature. Several approaches have been proposed in a previous publication to mitigate these two influences [27]. The approaches will be summarized briefly in following paragraphs.

### 3.2.1 Keeping the solder away from high current density/hot-spot region

By adopting a thick Cu or Ni UBM, the solder is positioned at far distance from the high current density/hot-spot region. As shown in Figs. 4 and 6, the current density/hot-spot region extends several microns toward solder. By using a Cu or Ni UBM of more than 10  $\mu\text{m}$  thick, the solder will be distant from this region. However, this approach does not reduce the current crowding and hot-spot temperatures in the whole joint. Instead, the current crowding and hot-spot occur in the thick Cu or Ni UBM, and the two metals are much more resistive to EM than the solders are. Our simulation results show that the maximum current density in solder with a 20- $\mu\text{m}$ -thick Cu UBM would be reduced by at least 10 times than that with a thin-film UBM. The hot-spot temperature will be reduced greatly since the local current density in the solder is alleviated and the solder stays away from the Al trace, which is the major Joule heating source. Thus, the MTTF would increase significantly.

### 3.2.2 Spreading the current uniformly by adding a thin resistive layer

By adding a thin resistive layer between the UBM and the Al trace, the current would be forced to spread uniformly on the passivation opening. This approach will reduce the current crowding effect to a quarter when one adds a thin layer of material with a resistivity of 3000  $\mu\Omega\text{ cm}$ . Further, this approach could almost eliminate the current crowding effect when the resistivity is increased to above 30000  $\mu\Omega\text{ cm}$ . Figure 9(a) and (b) shows the current paths schematically with and without this thin resistive layer. Without this layer, majority of the current would drift down near the entrance point of the Al trace, whereas with this layer, it will be forced to drift farther in the Al trace before going down to the solder bump. Thus, the current crowding effect could be greatly reduced with the

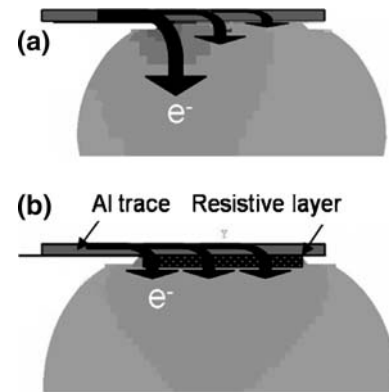


**Fig. 9** Schematic drawing showing the current path in the solder joints: (a) without and (b) with a thin resistive layer between the Al trace and the UBM

resistive layer. However, overlaying a resistive layer would inevitably increase the bump resistance, raising the Joule heating effect. Fortunately, the Joule heating effect is not significant at stressing current less than 0.2 A.

### 3.2.3 Decreasing the passivation opening

With smaller passivation opening, the current is likely to spread out rather uniformly before entering the solder bump, since the cross-section of the Al pad above the passivation opening is larger than that of the Al trace. The current crowding effect can be relieved by decreasing the diameter of the passivation opening. However, the Joule heating effect is not reduced but instead, it increases slightly because the current needs to drift longer in the resistive Al trace.

### 3.2.4 Enlarging the cross-section of the Al trace

Since the Al trace is the major source for Joule heating during accelerated EM test, enlarging its cross-section would produce a lower resistance. The heating power can be expressed as

$$P = I^2 R = j^2 \rho V \quad (2)$$

where  $P$  is the Joule heating power,  $I$  is the current,  $R$  is the resistance,  $j$  is the current density,  $\rho$  is the resistivity, and  $V$  is the volume. Therefore, the solder joints with a wider or thicker Al trace is likely to have lower Joule heating effect. Also, the current crowding effect will be relieved to some extent. In addition, the solder joint with a shorter Al trace will have lower Joule heating effect. But the current crowding effect remains the same. As the damascene Cu replaces Al metallization, solder joints with Cu trace will be



implemented in high-end consumer electronic devices shortly. It follows that the solder joints with the Cu trace would have lower Joule heating effect than that with an Al trace at identical configuration since the resistivity of Cu is only 63% of that of Al [28]. Yet, the current crowding effect remains almost unchanged when the Cu trace replace the Al trace with the same dimension.

Following the rational behind the discussion above and the technology available, the ideal solution for EM in solder joints would be Cu column [29]. Cu column up to 80  $\mu\text{m}$  thick can be fabricated as UBM in solder joint. A thin layer of solder is still required for the joint, as shown schematically in Fig. 10. Due the thick Cu layer, the current spreads out uniformly before reaching the solder. Therefore, there is almost minimum current crowding in solder. In addition, hot-spots in solder may also be eliminated completely due to negligible current crowding effect and superb thermal conductivity of Cu. Furthermore, during current stressing the solder may react with the Cu to form Cu–Sn IMCs. Since the amount of solder is much less than the Cu, the Cu column is unlikely to be consumed completely. Therefore, it may be one of the possible solutions for solder joint EM.

### 3.3 Investigating failure mechanism for thick-film UBM

Since thick Cu or Ni UBM have been adopted for Pb-free solder joints, the EM behavior and failure mechanism in those joints would be very important. However, only few studies have been performed on this topic [30, 31]. In particular, both electroplated and electroless Ni have been used as UBM materials due to

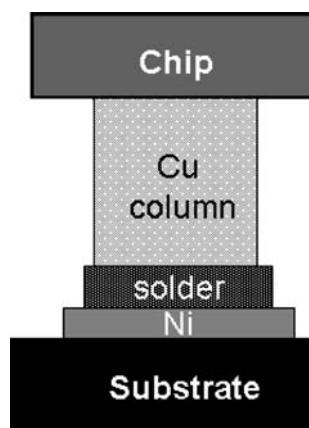


**Fig. 10** Schematic drawing showing a solder bump with a Cu column. This structure may be one of the solutions for EM in solder joints

their low reaction rate with solders [32]. Yet, the activation energy for Pb-free solder on the Ni UBMs has not been measured. Since the failure mechanism for Pb-free solder is primarily attributed to the dissolution of the UBM materials, the use of Ni UBM shall be able to inhibit the UBM dissolution rate, and thus to prolong the EM lifetime.

### 3.4 Thermomigration in Pb-free solders

As stated in previous section, the occurrence of thermomigration in Pb-free solders necessitates further investigations. As depicted in Fig. 8(b), the diffusion of Sn atoms from the substrate/cathode end to chip/anode end is enhanced by TM force for Bump 1. Possible void formation in Bump 1 under thermomigration is an interesting subject in our undergoing study.

### 3.5 Rotation of solder grains during EM

It has been demonstrated that Sn grains may rotate or grow during current stressing in Sn films, because white tin has anisotropic properties on electrical resistivity [33, 34]. It has a body-center tetragonal crystal structure with lattice parameters  $a = b = 0.583$  nm and  $c = 0.318$  nm, and its electrical resistivities are 13.25  $\mu\Omega$  cm and 20.27  $\mu\Omega$  cm, respectively. Thus, Sn grains may rotate during EM testing to reduce the total resistance of the Sn stripe. For Pb-free solders, the matrix consists of Sn grains. However, whether this phenomena would occur in solder bumps is not clear so far, and it needs further investigation.

## 4 Conclusions

Critical issues of EM in Pb-free solder joints have been reviewed. Our simulation results demonstrated that the distributions of current density and temperature remain almost the same when Pb-containing solders are replaced by Pb-free ones. Many researchers have reported that the EM lifetime for Pb-free solder is higher than that of the eutectic SnPb solders, but shorter than that of high-Pb solders. The underlying reason may be the low melting temperature, as electrical and thermal characteristics of solder bumps during EM testing, are quite similar. Several approaches have been suggested to relieve the current crowding and Joule heating effects in the solder bumps. Among them, thick UBM may be the most effective method to reduce the current crowding effect, whereas the reduction in the resistance of the Al trace would render significantly lower Joule heating. The solder

joints with Cu column is likely to be the ideal structures with highest EM resistance.

**Acknowledgements** The authors would like to thank the National Science Council of R.O.C. for financial support of this study through Grant No. 94-2216-E-009-021. In addition, simulation assistance from the National Center for High-performance Computing (NCHC) in Taiwan is appreciated.

## References

1. K.N. Tu, J. Appl. Phys. **94**, 5451 (2003)
2. H.B. Huntigton, A.R. Grone, J. Phys. Chem. Solids **20**, 76 (1961)
3. K. Zeng, K.N. Tu, Mater. Sci. Eng. Rep. **R38**, 55 (2002)
4. S. Brandenburg, S. Yeh, in *Proceedings of Surface Mount International Conference and Exhibition, SM198*, San Jose, CA, 23–27 August 1998, p. 337
5. C.Y. Liu, C. Chen, K.N. Tu, J. Appl. Phys **88**, 5703 (2000)
6. Q.T. Huynh, C.Y. Liu, C. Chen, K.N. Tu, J. Appl. Phys. **89**, 4332 (2001)
7. E.C.C. Yeh, W.J. Choi, K.N. Tu, P. Elenius, H. Balkan, Appl. Phys. Lett. **80**, 580 (2002)
8. T.L. Shao, S.-W. Liang, T.C. Lin, C. Chen, J. Appl. Phys. **98**, 044509 (2005)
9. S. H. Chiu, T.L. Shao, C. Chen, D.J. Yao, C.Y. Hsu, Appl. Phys. Lett. **88**, 022110 (2006)
10. H. Ye, C. Basaran, D. Hopkins, Appl. Phys. Lett. **82**, 7 (2003)
11. A.T. Huang, A.M. Gusak, K.N. Tu, Y.-S. Lai, Appl. Phys. Lett. **88**, 141911 (2006)
12. Y.H. Lin, Y.C. Hu, C.M. Tsai, C.R. Kao, K.N. Tu, Acta Mater. **53**, 2029 (2005)
13. J.W. Nah, K.W. Paik, J.O. Suh, K.N. Tu, J. Appl. Phys. **94**, 7560 (2003)
14. J. D. Wu, C.W. Lee, P. J. Zheng, J. C.B. Lee, S. Li, in *Proceedings of the 54th Electronic Components and Technology Conference*, IEEE Components, Packaging, and Manufacturing Technology Society, Las Vegas, NV, 2004, p. 961
15. S. Gee, N. Kelkar, J. Huang, K. N. Tu, in *Proceedings of IPACK2005, ASME InterPACK 2005*, San Francisco, CA, USA, 2005
16. W.J. Choi, E.C.C. Yeh, K.N. Tu, J. Appl. Phys. **94**, 5665 (2003)
17. T.L. Shao, S.H. Chiu, C. Chen, D.J. Yao, C.Y. Hsu, J. Electron. Mater. **33**(11), 1350 (2004)
18. Y.-S. Lai, K.M. Chen, C.W. Lee, C.L. Kao, Y.H. Shao, in *Proceedings of EPTC 2005, 7th Electronics Packaging Technology Conference*, Singapore, 2005, p. 786
19. T.Y. Lee, W.J. Choi, K.N. Tu, J.W. Jang, S.M. Kuo, J.K. Lin, D.R. Frear, K. Zeng, J.K. Kivilahti, J. Mater. Res. **17**(2), 291 (2002)
20. A.A. Liu, H.K. Kim, K.N. Tu, P.A. Totta, J. Appl. Phys. **80**(5), 2774 (1996)
21. S.W. Chen, C.M. Chen, W.C. Liu, J. Electron. Mater. **27**(11), 1193–1198 (1998)
22. T.L. Shao, Y.H. Chen, S.H. Chiu, C. Chen, J. Appl. Phys. **96**(8), 4518 (2004)
23. Y.H. Chen, T.L. Shao, P.C. Liu, C. Chen, T. Chou, J. Mater. Res. **20**(9), 2432–2442 (2005)
24. G.A. Rinne, Microelectron. Reliab. **43**, 1975 (2003)
25. S.H. Chiu, S.W. Liang, C. Chen, D.J. Yao, Y.C. Liu, K.H. Chen, S.H. Lin, in *Proceedings of the 56th Electronic Components and Technology Conference*, IEEE Components, Packaging, and Manufacturing Technology Society, San Diego, CA, 2006
26. J.R. Black, IEEE Trans. Electron. Devices ED **16**(4), 338 (1969)
27. S.W. Liang, T.L. Shao, C. Chen, E.C.C. Yeh, K.N. Tu, J. Mater. Res. **21**(1), 137 (2006)
28. C.Y. Hsu, D.J. Yao, S.W. Liang, C. Chen, J. Electron. Mater. **35**, 947 (2006)
29. J.W. Nah, J.O. Suh, K.N. Tu, S.W. Yoon, C.T. Chong, V. Kripesh, B.R. Su, C. Chen, in *Proceedings of the 56th Electronic Components and Technology Conference*, IEEE Components, Packaging, and Manufacturing Technology Society, San Diego, CA, 2006
30. Y.H. Lin, C.M. Tsai, Y.C. Hu, Y.L. Lin, C.R. Kao, J. Electron. Mater. **34**(1), 27 (2005)
31. J.K. Lin, J.W. Jang, J. White, in *Proceedings of the 53th Electronic Components and Technology Conference*, IEEE Components, Packaging, and Manufacturing Technology Society, New Orleans, USA 2006, p. 816
32. P.G. Kim, J.W. Jang, T.Y. Lee, K.N. Tu, J. Appl. Phys. **86**, 6746–6751 (1999)
33. A.T. Wu, A.M. Gusak, K.N. Tu, C.R. Kao, Appl. Phys. Lett. **86**, 241902 (2005)
34. A.T. Wu, J.R. Lloyd, N. Tamura, B.C. Valek, K.N. Tu, C.R. Kao, Appl. Phys. Lett. **85**(13), 2490 (2004)